JET–P(98)68

G A Cottrell et al

Evolution of Internal Transport Barriers in JET Optimised Shear Plasmas

JET–P(98)68

Evolution of Internal Transport Barriers in JET Optimised Shear Plasmas

G A Cottrell, Y F Baranov, C D Challis, C Gormezano, A Ekedahl, G T A Huysmans, X Litaudon, D O'Brien, F Rochard, G J Sadler, P Schild, A C C Sips, F X Söldner, B J D Tubbing, D J Ward, W P Zwingmann.

JET Joint Undertaking, Abingdon, Oxfordshire, OX14 3EA,

Preprint of a Paper to be submitted for publication in the proceedings of the Satellite Workshop of 1998 EPS

January 1999

ABSTRACT

High performance discharges with optimised magnetic shear having a broad or hollow current density profile have been produced in JET. These plasmas are characterised by improved core confinement within a region called the Internal Transport Barrier (ITB). Near the plasma centre, the ion thermal diffusivity is reduced to levels close to the standard neo-classical level in both D-D and D-T plasmas. With D-D fuel, a JET record neutron yield ($R_{NT} = 5.6 \times 10^{16}$ s^{-1}) was produced and, with D-T fuel, L-mode discharges with 7.2 MW of fusion power, and H-mode discharges with up to 8.2 MW of fusion power are obtained. Central ion temperatures approaching 40 keV, ion temperature gradients of 150 $keVm^{-1}$ and plasma pressure gradients of 10^6 Pa m^{-1} are observed in D-T leading to a fusion triple product $n_i T_i \tau_E = (1.1 \pm 0.2) \times 10^{21}$ m^{-3} keVs. Central toroidal rotation frequencies up to 37 kHz are observed and the rotational flow near the radius of the ITB is strongly sheared. These plasmas are prepared by applying Lower Hybrid Current Drive (LHCD) and Ion Cyclotron Resonance Heating (ICRH) during the early current ramp-up phase, "freezing-in" a flat or possibly slightly hollow current density profile; into this target the main heating, consisting of combined Neutral Beam Injection (NBI) and ICRH, is applied. By superposing an ITB with an edge barrier (ELMy H-mode), near steady-state conditions (H-89 $\approx$ 2 for four energy confinement times) with high fusion yield have been achieved, offering a possible route towards quasi-steady-state. High fusion yield, quasi-steady-state plasmas with confinement significantly above the standard sawtoothing ELMy H-mode can be achieved in this way. The techniques previously developed with D-D plasmas were modified to allow an L-mode ITB to form in D-T with a lower L to H-mode power threshold. The heating power and the *q*-profile were similar in both cases. ICRH plays a key role in the direct heating of core ions which allows real-time control of the central pressure profile.

1. INTRODUCTION

A major part of the present development of thermonuclear fusion power in tokamaks is the exploration of methods to reduce energy losses from the plasma core. Improvements in fusion performance can be made by optimising the kinetic pressure profile - within the boundaries imposed by MHD stability. In standard H-mode edge barrier plasmas, a thermal transport barrier forms in a narrow radial region just inside the magnetic separatrix, giving rise to a characteristically steep edge pressure gradient which is associated with the relaxation phenomena of edge-localised MHD modes (ELMs). High fusion performance can be obtained transiently in the H-mode ELM-free regime; however, eventually the edge pressure gradient becomes sufficiently large to destabilise ballooning MHD modes which ultimately limit steady-state fusion performance. H-mode discharges with continuous ELM activity present offer better prospects for steady-state performance, however in this case the global fusion performance is reduced.

The main problem with the standard hot-ion H-mode regime is that the core transport is significantly faster than transport though the edge transport barrier. The result of this is an early loss of of the MHD stability at the plasma edge while the core plasma is still far from being either kink and ballooning unstable. In H-mode discharges the central plasma pressure is also limited by MHD sawteeth as well as by other MHD activity, such as neo-classical tearing modes. To improve the performance of the hot-ion H-mode, one therefore must seek ways to reduce the core transport as well as that at the edge, by allowing an internal transport barrier (ITB) to co-exist with the edge H-mode barrier. With the higher core ion pressures produced inside an ion ITB the fusion reactivity is enhanced. Establishing an electron internal transport barrier is also important since, in a fusion reactor burning D-T fuel, the alpha-particle heating efficiency can be increased inside the ITB by locally reducing the electron conductive and convective losses.

To improve central plasma performance, sawteeth can be avoided for some time by operating the tokamak with a value of the central safety factor, $q(0) > 1$, a regime that can be accessed by applying additional heating during the current rise phase. Improved central confinement and high performance have both been demonstrated on JET by central pellet fuelling of sawtooth-free discharges combined with intense central heating [1]. The central magnetic shear ($s = r/q(\mathrm{d}q/\mathrm{d}r)$) in these discharges was low and possibly negative [2]. A number of other tokamak devices (TFTR [3], DIII-D [4] and JT60 [5]) have recently reported the formation of internal transport barriers using neutral beam injection (NBI) auxiliary heating during the current rise. All have demonstrated improvements in the central confinement and in fusion performance with the formation of a high temperature and high density core plasmas.

The use of ICRH, available on JET in addition to NBI, adds a second additional heating system which has been used to explore further the improved regimes. Radiofrequency (RF) power is used to excite a fast magnetosonic wave, to which the high density plasma core is accessible. The wave is absorbed at a cyclotron resonance which is positioned in major radius (usually the plasma centre) by the choice of magnetic field and RF frequency. ICRH performs three key roles in these discharges. In the preheating phase it delays the current penetration, during the formation time of the internal transport barrier it produces steep pressure gradients near the plasma centre, and, during the growth phase of the internal transport barrier, it supplements the central ion heating and helps to maintain the steep ion pressure gradient. When high power combined ICRF and NBI heating is applied to JET plasmas during the early current rise phase (the optimised shear regime), the central plasma confinement is observed to improve when the magnetic shear in the central region is close to zero [6 - 10]. ITB discharges with improved fusion reactivity have been obtained in the JET ELM-free regime as well as in the ELM-ing regime - the so-called “double barrier” regime. In these cases the peaking of pressure profile is limited by pressure-driven MHD kink modes [11].

2. SCENARIO FOR THE JET OPTIMISED SHEAR REGIME

Theory predicts that turbulent cross-field energy transport will be reduced in plasmas with low or reversed magnetic shear. However, in standard (un-optimised magnetic shear) tokamak plasmas, the ohmic current density profile naturally tends to peak on axis lowering $q(0)$. To broaden the current density profile for some time, we have therefore prepared target plasmas in JET by applying additional heating (primarily of electrons) during the current ramp-up phase which increases the poloidal field diffusion time and delays current penetration. This produces a low central magnetic shear plasma target with $q(0) > 1$. Once suitable target plasma conditions are achieved, the additional heating power is increased strongly to produce a plasma with a steep ion pressure gradient and sheared rotational flow. These conditions lead to low energy transport coefficients inside an ITB [12]. As the pressure gradient increases, the bootstrap current increases to provide approximately 30 % of the plasma current off-axis. The maintainance of an optimum magnetic configuration in steady-state is a problem for which the use of non-inductive current profile control is eventually seen as a permanent solution. A summary of the JET Optimised Shear discharges analysed in this paper is given in the Table.

Pulse	Gas	PRF	PNBI	Comments
40542	DD	6.0 MW	19.5 MW	ITB + Elmy H-mode edge; quasi-steady-state
40554	DD	6 MW	18.7 MW	Highest performance DD pulse. BT = 3.4 T
40847	DD	6.1 MW	19 MW	ne peaked
42426	DD	6.2 MW	18.2 MW	BT = 3.8 T.
42733	DT	6.1 MW	(D) 8.1 MW (T) 10.3 MW	ITB + Elmy edge
42746	DT	6.1 MW	(D) 9.2 MW (T) 7.2 MW	Highest performance DT pulse. BT = 3.4 T
42982	DT	3 MW	(D) 11 MW (T) 10.6 MW	Reference to 42733; Elmy H-mode edge

The scenario for ITB Production was developed first in D-D plasmas and then found, with some modifications, to be directly applicable in D-T plasmas. Generally, the early triggering of an ITB, soon after application of the main heating, gave the highest subsequent fusion performance. The central problem in the D-T plasma development work was the lower L- to H-mode power threshold [13] which meant that careful tuning of waveforms was needed to avoid a premature transition to the H-mode. In D-T plasmas, ITBs formed at similar NBI power levels

and *q*-profiles. The T / T+D concentration achieved was ~ 35%.

Fig. 1 shows the typical ITB scenario in a D-D plasma (pulse 42426) with a toroidal field of B_T=3.8 T. A short pulse of low power LHCD is used during the plasma breakdown time t = 2 s to assist reliable plasma formation. In the preheating phase (before t = 5 s), 1 MW of central ICRH is applied and the target central electron density is 1.5×10^{19} m^{-3}. The main heating is applied at t = 5.5 s consisting of up to 17.5 MW of NBI power and 6.0 MW of central ICRH power applied in ramp-up phase of the plasma current. An L-mode ITB formed after this time and the peak values of diamagnetic stored energy (W_{dia}= 12.5 MJ), central electron density ($n_e(0)$ = 6×10^{19} m^{-3}) and central ion temperature ($T_i(0)$ = 32 keV) are achieved. The peak central electron temperature is $T_e(0)$ =13 keV and the peak D-D neutron rate R_{NT} is 5.6×10^{16} s^{-1}. An ELM-free H-mode forms from 6.68 s until 7.1 s when the high performance phase is terminated by a giant ELM.

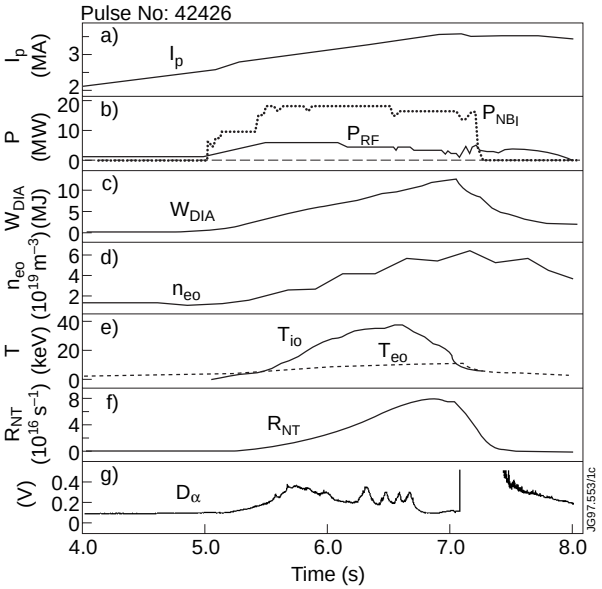

Figure 1. Overview of JET high performance optimised shear pulse No. 42426 showing the ramp-up phase of the plasma current (trace a*) during which combined deuterium neutral beam injection ($P_{NBI} \leq 17.5$ MW) and central ICRH ($P_{RF} \leq 6.0$ MW) was applied (trace* b*). Trace* c *shows that the diamagnetic stored energy reached a peak value of W_{dia}= 12.5 MJ at time 7 s. Traces (*c*) and (*d*) show the central values of electron density, ion and electron temperatures reach peak values of $n_{e0} = 6 \times 10^{19}$ m^{-3} , T_{i0} = 32 keV and T_{e0} =13 keV. The total DD and DT neutron emission (trace* f*) reaches a maximum rate of R_{DD}+ R_{DT} = 8.1×10^{16} s^{-1}, of which R_{DD}= 5.6×10^{16} s^{-1} was from DD fusion reactions. The intensity of D_α emission is shown in trace* g.

3. EVOLUTION OF PLASMA PROFILES AND THE ITB

The evolution of the electron density profile is shown in Fig. 2. The target plasma is shown at t = 5.3 s when the neutral beam power is P_{NBI} = 8 MW. An ITB forms 100 ms after application of the full heating power at t ~ 5.6 s. The ITB expands to a normalised radius of ρ_{ITB} ~ 0.55 at t ~ 6.7 s; with central fuelling from NBI, the density becomes peaked with $n_e(0)$ reaching up to 6×10^{19} m^{-3}. When the ELM-free H-mode triggers (at t = 6.68 s), the edge $n_e(a)$ increases sharply and the density peaking is maintained into the H-mode phase up to the time of the giant ELM. The peak fusion performance is reached at t = 7.0 s.

The evolution of the ion temperature, angular rotation and plasma pressure profiles is shown in Figs. 3-5. Each of these quantities becomes peaked inside the ITB. During the L-mode phase, early steep gradients form in an radially expanding region of low particle and thermal transport. In this pulse, central toroidal rotation frequencies up to 32 kHz are observed and the rotational flow near the radius of the ITB is strongly sheared in the interval $0.4 < \rho < 0.6$.

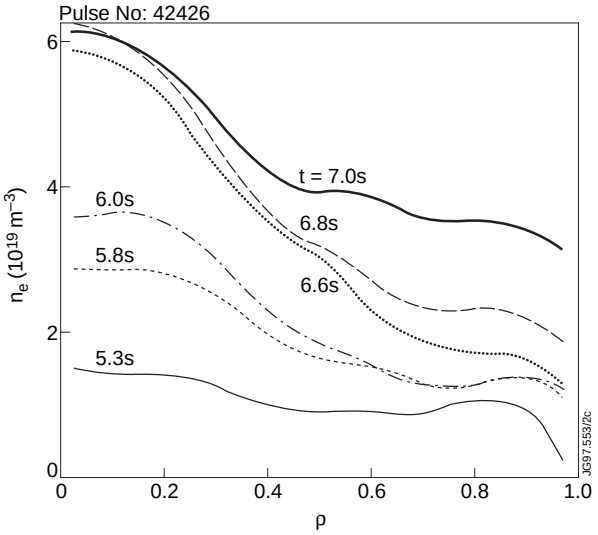

Figure 2. Evolution of LIDAR profiles of electron number density mapped onto the normalised radial co-ordinate, ρ, with the TRANSP code equilibrium. Note the strong peaking of the density which occurred during the L-mode phase (time t ≤ 6.6 s) which persisted into the H-mode phase (time t ≥ 6.68 s) at which time the density at the edge increased sharply.

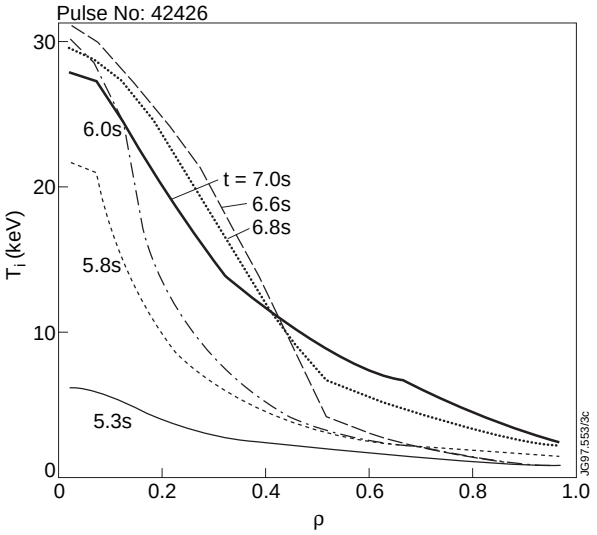

Figure 3. Evolution of the ion temperature profile (from charge-exchange recombination measurements) mapped onto the normalised radial co-ordinate, ρ, with the TRANSP code equilibrium. Note the early presence of a steep gradient region which expanded radially with time indicating the formation of a region of low transport (internal transport barrier).

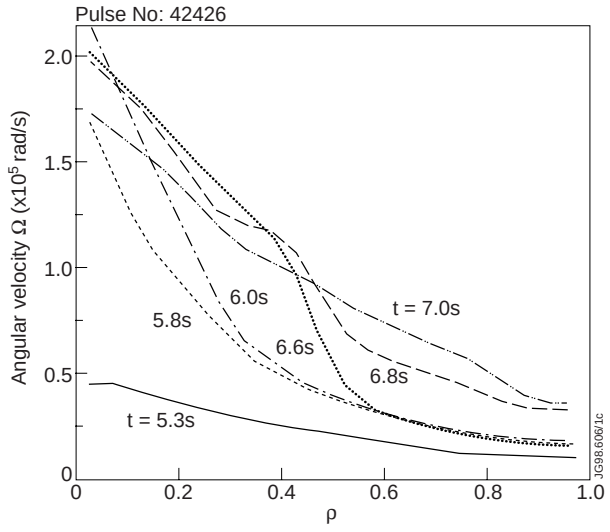

Figure 4. Evolution of the angular rotation profile (from charge-exchange recombination measurements) mapped onto the normalised radial co-ordinate, ρ,. Note the early presence of a steep gradient region which expanded radially with time indicating the formation of a region of low momentum transport.

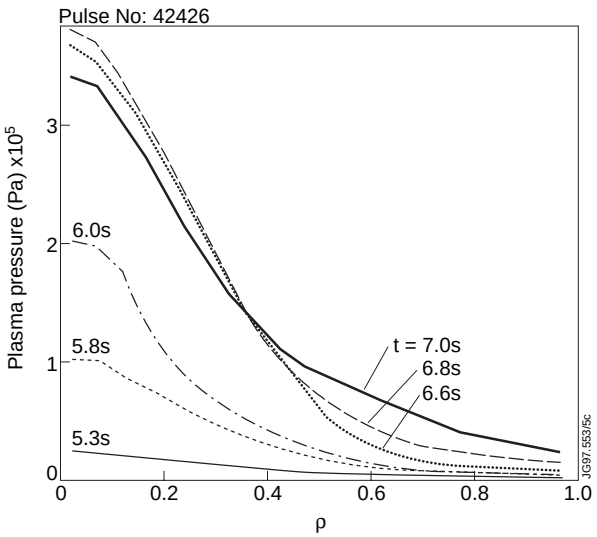

Figure 5.Evolution of the plasma pressure profile showing the formation of a steep gradient region that moved radially outwards with time during the L-mode phase. The maximum central pressure ($p_0 = 3.8 \times 10^5$ Pa) was attained near the time of the LH transition (time t = 6.68 s) after which the inner (ρ ≤0.4) pressure gradient decreased and the outer (ρ ≥0.4) pressure gradient increased.

Peak central values of $T_i(0)$ = 32 keV and plasma pressure p(0) = 4 bar are achieved. The ion ITB footpoint is revealed in the plot of the contours of $\nabla^2 T_i$; the ITB footpoint radius follows the line of the maximum in Fig. 6. Between t = 5.5 s to 6.5 s, the ITB expands at a rate of

approximately 0.5 m s^{-1}. At time 6.68 s, the gradients inside ρ ~ 0.4 decrease and those outside increase indicating the formation of an outer (edge) ELM-free H-mode transport barrier.

The *q*-profile (Fig. 7) was reconstructed initially with the EFIT equilibrium during the low-β phase of the discharge and then allowed to evolve during the high-β phase using the TRANSP equilibrium solver, including the effects of the plasma pressure profile and the non-inductive beam-driven and bootstrap currents. The rate of current diffusion was calculated classically. Up to time of the main heating *q* remains above two and increases monotonically with radius. However, at the time of the ITB formation (t = 5.6 s), *q* flattens around ρ = 0.25 with *q* ~ 2. The ITB grows with the *q*=2 surface in the plasma. Subsequently, there is possibly a weak shear reversal. At the time of peak performance, $q < 2$ inside ρ ~ 0.55 with a minimum $q_{min}(0.43) \sim 1.9$.

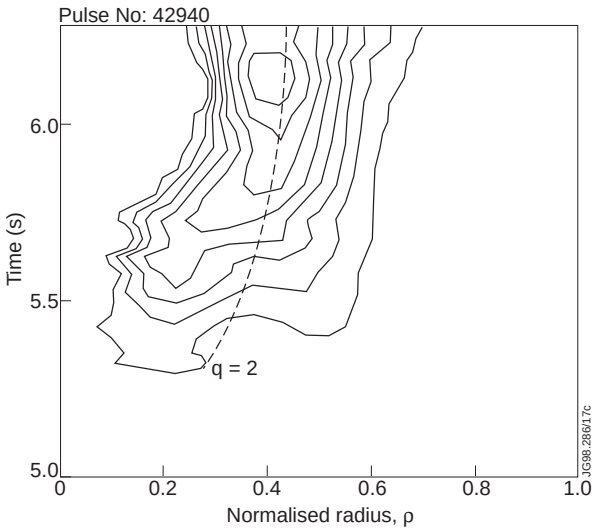

Figure 6.Evolution of the position of the 'footpoint' of the internal transport barrier revealed as contours of $\nabla^2 T_i$ in the time-normalised radius plane for a toroidal field B_T = 3.8 T deuterium-tritium pulse (No. 42940) which produced a fusion power of 7.2 MW in the L-mode phase. The position of the q = *2 magnetic surface, computed using the TRANSP code, is indicated by the dashed line.*

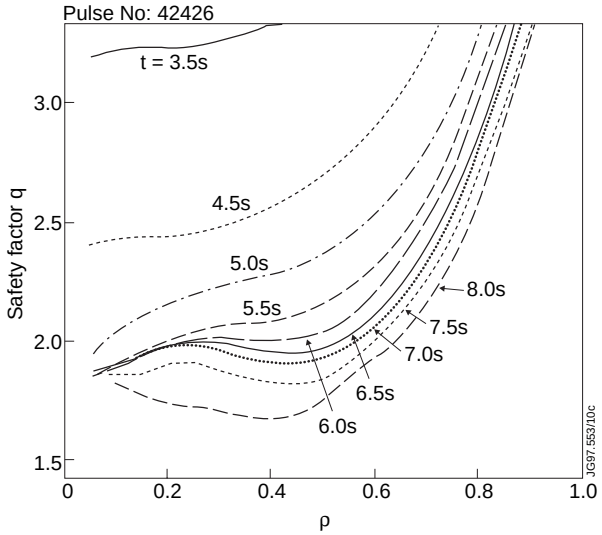

Figure 7. Evolution of the safety factor profile from combined TRANSP and EFIT reconstruction. This reconstruction is consistent with the formation of a region of negative shear during the high performance (ITB) phase of the discharge.

The breakdown of the total current from TRANSP calculation is shown in Fig. 8 with current density profiles shown in Figs. 9 and 10. During the early ITB phase the current density profile, j(r), is flattened in the central region by the beam-driven current. As the plasma density builds up inside the ITB, this current is decreased in magnitude. During the later ITB phase, j(r) continues to be flattened in the central region by the bootstrap current. The total bootstrap current constitutes up to 30% of the total plasma current.

Fig. 11 shows that the footpoints of T_i , ion thermal diffusivity, χ_i , momentum diffusivity, χ_ϕ, and n_e are aligned (within $\Delta\rho \approx 0.1$) with each other. Also plotted is the evolution of the calculated *q* = 2 rational surface which aligns well with the plasma footpoints.

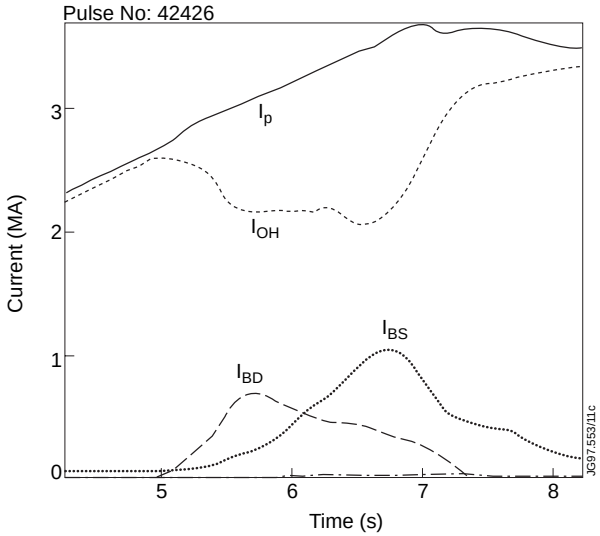

Figure 8. Composition of the total plasma current. Total current: I_p ; ohmic current: I_{OH}; beam-driven current : I_{BD}; and bootstrap current: I_{BS}.

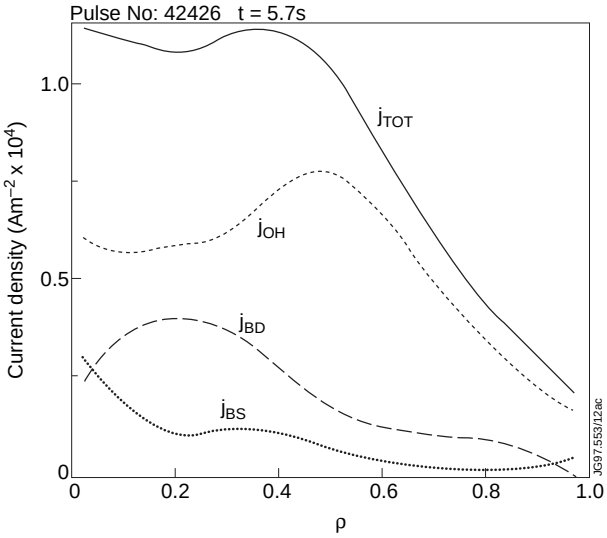

Figure 9. Current density profiles at time t = *5.7 s. Total current density: j_{TOT}, ohmic current density: j_{OH}, bootstrap current density: j_{BS}, and beam-driven current density: j_{BD}.*

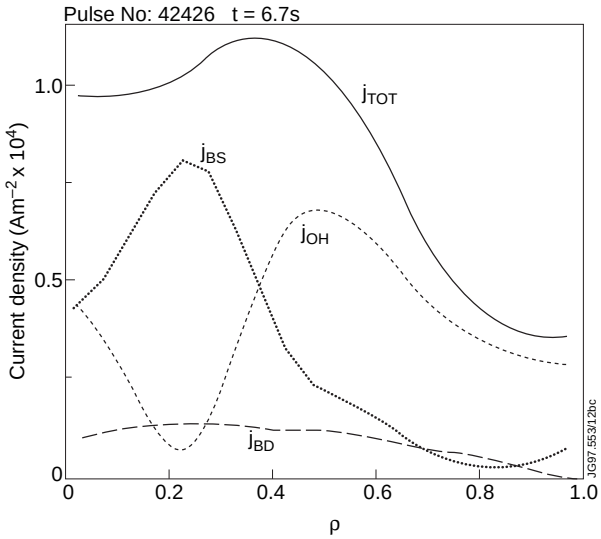

Figure 10. Current density profiles at time t = *6.7 s when the bootstrap current reaches a maximum value.*

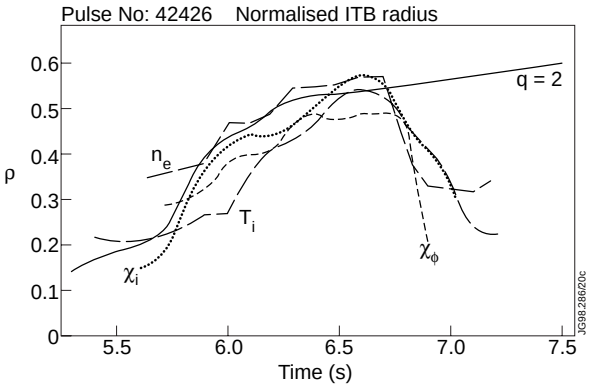

Figure 11. ITB footpoint radii of various quantities.T_i; ion temperature; χ_i : ion thermal diffusivity; χ_ϕ : angular momentum diffusivity, and n_e : electron density. These are plotted with the radius of the q=*2 rational surface.*

4. DIRECT ICRH ION HEATING OF THE ITB

Central ICRF heating [14] with π /2 phasing and frequency f = 51.2 MHz ($\omega = \omega_{cH} = 2\omega_{cD}$) was applied in pulse No. 40554. The RF power absorbed by the various species is shown in Fig. 12. In this calculation a bounce-averaged Fokker-Planck model in the TRANSP code was used, which included the computation of the RF power damped on the injected deuterium ions at second harmonic resonance, $\omega = 2\omega_{cD}$, and the resultant distortion of the beam distribution due to this interaction. The split of the damped RF fast wave power between deuterium (P_D) and

hydrogen (P_H) ions depends on the concentration of minority particles: $\eta = n_H / (n_H + n_D)$ in the central resonance layer and is given by the approximate relation [15]

$$\frac{P_D}{P_H} \propto \frac{\beta_D}{\eta} \tag{1}$$

where β_D is the beta value of the deuterium ions. Thus, for a given minority concentration, the fast wave power damped on the ions increases in proportion to the core ion pressure. In the modelling, the calculated value of diamagnetic stored energy, W_{dia}, is largely insensitive to the assumed value of η, but the calculated D-D neutron rate, R_{NT}, is sensitive to this parameter [16, 17]. Both PION and TRANSP models are able to obtain good agreement between the calculated and measured D-D neutron rate, R_{NT}, assuming a fixed concentration of $\eta = 3$ % in pulse No. 40554. For reference, the effect of assuming a lower value $\eta = 1.6$ % in pulse A is also shown in Fig. 12. Reducing the minority concentration lowers the total RF power absorbed on the minority ions and increases the power absorbed on the deuterium ions, by approximately 1 MW. With $\eta = 1.6$ %, the total predicted D-D neutron emission rate from the plasma increased by 8%, which lies just within the measurement error band.

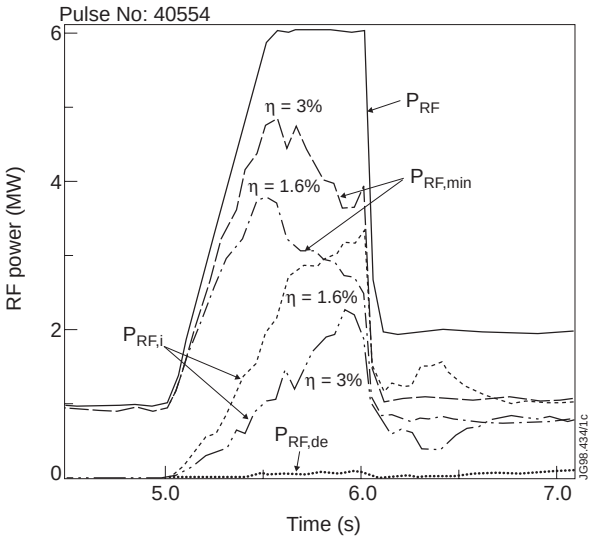

Figure 12. RF power absorbed by the various species for pure deuterium pulse No. 40554. The traces are: total coupled RF power (P_{RF}), power absorbed by minority H ions ($P_{RF,min}$), RF power absorbed directly by D ions and RF power absorbed directly by thermal electrons ($P_{RF,de}$). Two cases are shown with assumed hydrogen minority concentrations of 3% and 1.6%.

As the coupled RF power, P_{RF}, is ramped up (from t = 5 s to 5.5 s), the power absorption takes place predominantly on the hydrogen minority ions. At $t \sim 5.5$ s, with the formation of an internal transport barrier and the build-up of energetic injected deuterium ion density, the central pressure of deuterium ions, $\beta_D(0)$ increases to a level where $2\omega_{cD}$ damping ($P_{RF,i}$) in the hot core becomes significant with respect to the local ion energy balance and comparable with the minority damping ($P_{RF,min}$). Of the RF power coupled to the deuterium, most went to the injected beam ions having energies $E > 3/2\ T_i$, and only a relatively small amount to the thermal deuterons with energies $E < 3/2\ T_i$. The average energy of the NBI deuterons, $\langle E_{NBI} \rangle$, perturbed by the RF interaction, increases the average energy of the NBI deuterons by typically a few tens of keV in the central part of the plasma $\rho < 0.25$. The relatively modest increase in $\langle E_{NBI} \rangle$ is insufficiently large to produce a strong deuterium tail (which could have enhanced the D-D beam-thermal fusion rate in the plasma centre [16], and led to data inconsistencies). The perturbed deuterium population still has an average energy lying significantly below the

critical energy where fast ions experience equal ion-ion and ion-electron friction [18]. In the example shown, $E_{crit}(0) \sim 190$ keV. The ratio of NBI ion to electron heating power is therefore not strongly affected by the RF interaction and still remains weighted strongly towards ion heating.

5. DOUBLE TRANSPORT BARRIERS - QUASI-STEADY STATE

In the discharges described above, an ITB forms during the L-mode phase and, after a period of core pressure evolution in which most of the enhancement in performance occurs in the plasma core, an ELM-free H-mode is triggered in which the inner pressure gradient weakens and the edge pressure gradient steepens. Eventually the edge pressure gradient reaches the MHD ballooning limit and the high performance phase is terminated by a giant ELM. This route does not permit steady-state operation. However, if the ITB is superposed on an ELMy H-mode with appropriate edge conditions, the frequent small ELMs continually relax the edge pressure gradient, allowing a possible route to quasi-steady-state operation with a combination of edge and internal transport barriers. We have performed initial experiments in this so-called "double barrier" regime to attempt to further optimise the plasma pressure profile and explore the potential for possible quasi-steady-state operation. Examples [19] are shown in Fig. 13, comparing D-T pulse 42733 (optimised shear plus ELMy H-mode type) with pulse 42982 (standard ELMy H-mode type). In pulse 42733, the NBI power was stepped down for neutron economy. In this double barrier pulse, the ELMy H-mode edge conditions persisted until the NBI step-down

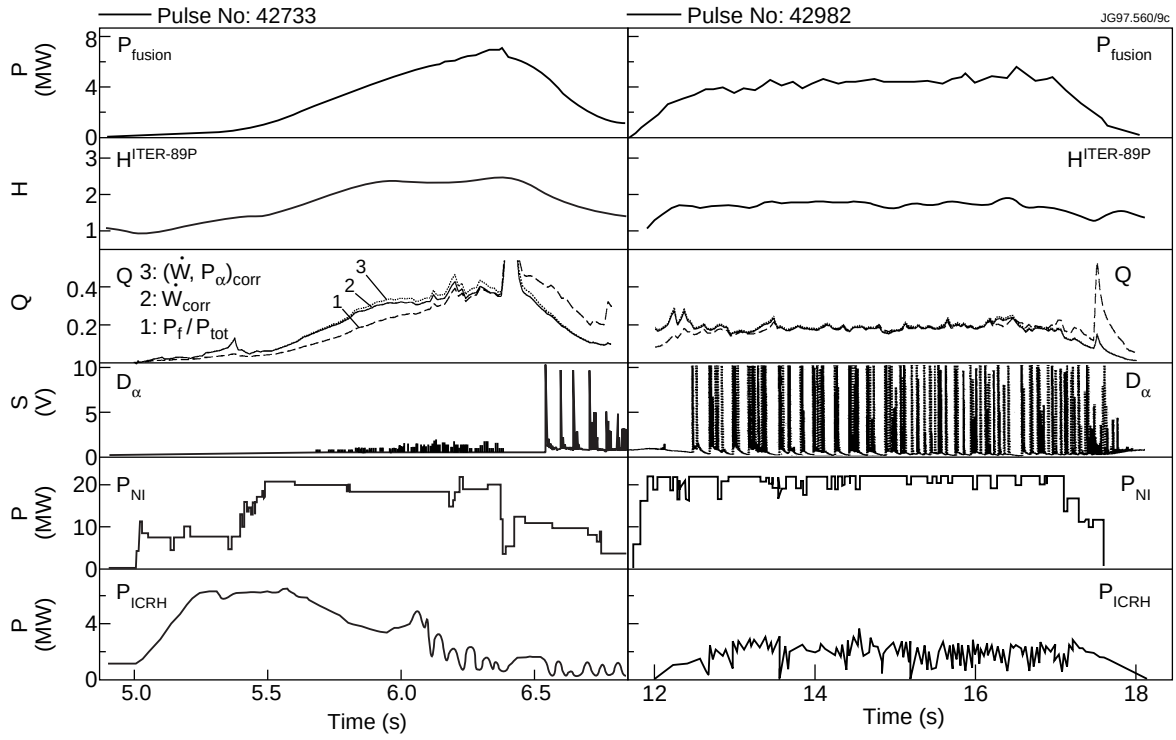

Figure 13. Comparison of the "double barrier" D-T pulse No. 42733 with the standard ELMy H-mode D-T pulse No. 42982.

time. The ITER H89-P normalised confinement factor was higher (reaching 2.2) than in the reference pulse (reaching approximately 1.8) and the D-T fusion power reached approximately 7 MW, compared with approximately 4 MW in the reference pulse. The fusion gain, Q, was higher also, reaching approximately 0.4, compared with 0.25 in the reference pulse.

Another example of the double barrier regime in which the NBI power was applied for a longer duration is shown in Fig.14 for D-D fuelling. The ITB forms shortly after the step-up in the NBI power at time t = 5.4 s, an H-mode is triggered at time 6.15 s, and the ELMy H-mode edge persists throughout the main heating pulse until the NBI step-down at time 7.5 s. In this case the confinement was maintained at a level of H89-P ~ 2 for four energy replacement times. Both of these examples indicate that the double barrier regime offers promise for establishing quasi-steady-state enhanced performance discharges [19] .

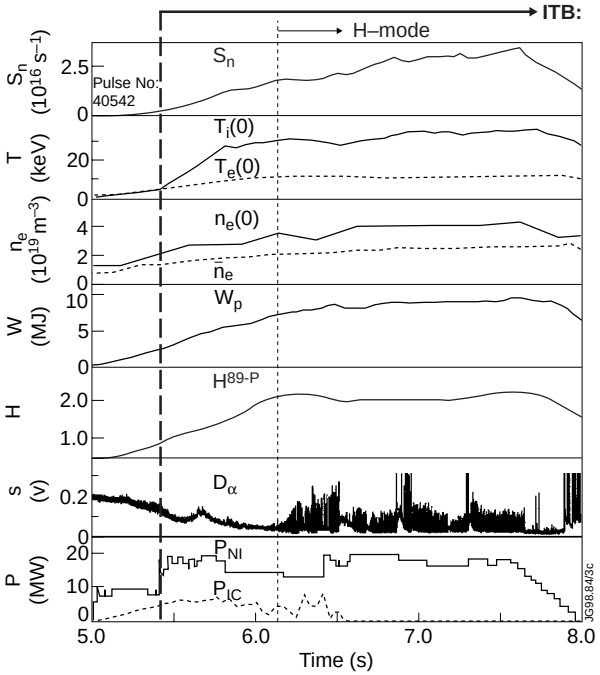

Figure 14. A "double barrier" D-D pulse No. 40542 in quasi-steady conditions.

6. ENERGY BALANCE AND TRANSPORT COEFFICIENTS

The TRANSP code was used to determine the evolution of the plasma energy transport coefficients, particularly in the ion heat loss channel which is dominant in these discharges. A comparison is made between the measured ion thermal diffusivity the standard neoclassical ion thermal diffusivity [20]. Typical JET optimised shear plasmas are characterised by high central values of ion temperature and low central poloidal field. The thermal ion banana widths can become large and comparable with typical length scales near the plasma centre. This means that the comparison between computed χ_i values and the standard neoclassical ($\chi_{i,neo}$) values becomes increasingly uncertain as the centre of the plasma is reached [21]; in our case this occurs typically inside a normalised radius of $\rho < 0.15$. With the formation of the ITB, the strongest improvement in the transport coefficients was found to be in the ion thermal diffusivity, χ_i . On formation of the ITB, χ_i decreases initially in the centre of the plasma and this is then followed by a region of reduced χ_i which expands radially, following a trajectory inside the footpoint of the ITB. Fig. 15 shows the comparison of the profiles of ion thermal diffusivity (measured and standard neoclassical) of D-D and a D-T ITB discharges. The presence of the ITB decreases χ_i by about an order of magnitude. In the central region of the plasma, near-neoclassical levels of ion energy transport are indicated. This conclusion is independent of the D-D or D-T fuelling.

An electron ITB [22] also forms (Fig. 16) in these discharges and its position and expansion rate agrees well those of the ion ITB. A reduction, by a factor of typically 2, in the electron thermal diffusivity, χ_e , is also observed from transport studies.

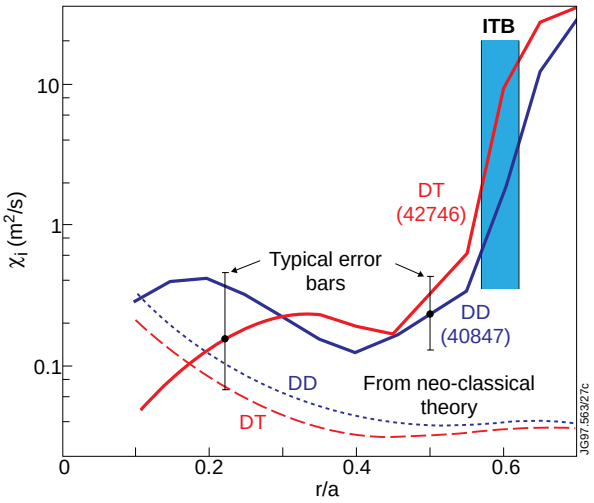

Figure 15. Plot of the profiles of the ion thermal diffusivity, χ_i , at various radii for pure D-D and D-T pulses

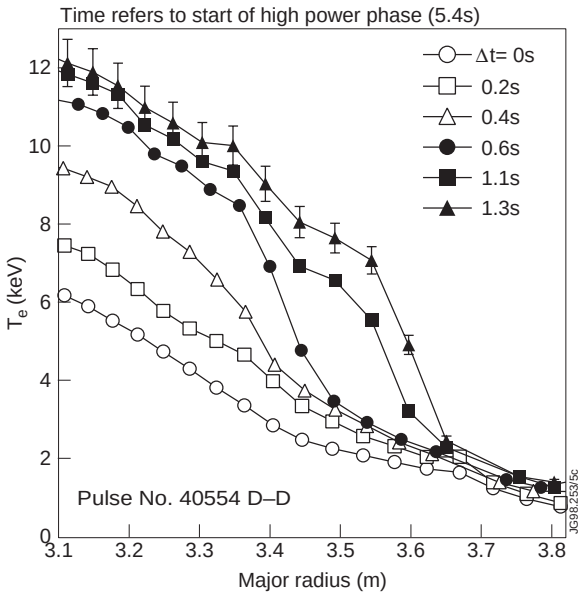

Figure 16. Evolution of the electron temperature profiles; for pulse No. 40554.

7. DISCUSSION

The physics underlying the formation of the ITB is not well understood at present. Different theoretical ideas of the ITB formation include: the stabilisation of trapped electron and ballooning mode turbulence by negative magnetic shear, turbulence stabilisation by a sheared plasma rotational flow, and a decoupling and suppression of the toroidally linked tubulence by a combination of low magnetic shear and a sheared plasma rotational flow. A predictive transport model [23] has been used to test the JET empirical transport model which is composed of a linear combination of Bohm, gyroBohm and neoclassical transport coefficients. Each of the three theoretical models was tested by choosing the method of choosing fitting parameters which premultiply the Bohm coefficient in the empirical transport model. If only the magnetic shear was included, an ITB is formed but there is no radial expansion, as observed experimentally. If, on the other hand, only a strongly sheared plasma rotational flow is included, an ITB forms with an expansion rate much faster than the experimental observation and the resulting ion temperature profile is too broad. The best agreement with the experimental time-varying plasma profiles is obtained using a model which combines a weak magnetic shear and a strongly sheared plasma rotational flow. In this model the ITB dynamics are well reproduced, in particular, the formation, expansion and the contraction (H-mode) phases. This modelling has yet to be completed for the electron ITB.

8. CONCLUSIONS AND SUMMARY

Recent experiments on the JET tokamak have demonstrated the triggering of ITBs in both D-D and D-T plasmas with similar power levels and plasma current profile with the main heating applied during the ramp-up of the plasma current. The ITB is found to be triggered when the magnetic q=2 surface appears in the plasma for D-D and in D-T plasmas. During the early ITB phase [14] the plasma energy content is dominated by fast ions with roughly half originating from ICRH energetic minority protons (with particle energies in the range of a few MeV) and the remainder from NBI ions (with particle energies in the range of 100 keV). During this phase, the ICRH energetic ions have large banana widths and precess around the torus forming a toroidal current which tends to flatten the current density profile and raise $q(0)$. In this early phase, the neutral beam-driven current also tends to flatten j(r). The footpoints of the rotation, electron density, electron and ion temperature ITBs form and evolve similarly, and expand at a rate ~ 0.5 m s^{-1} out to a maximum normalised radius of $\rho \sim 0.6$. Characteristic of the evolved ITB state is the strong peaking of the profiles of electron density (with central values up to 7×10^{19} m^{-3}), ion temperature (with central values up to 40 keV) electron temperature (with central values up to 14 keV) and plasma pressure (with central values up to 4 bar). MHD analysis shows the pressure profile to be limited by pressure-driven global n=1 kink modes [11].

In ITB plasmas with both D-D and in D-T fuelling, the ion thermal diffusivity is decreased to levels close to the standard neo-classical levels in the plasma core. In the later, more evolved ITB phase, the plasma energy content is predominantly thermal, comprising typically up to 70% of the total energy in the case of the more optimised D-D plasmas. At the peak fusion performance time, up to 50% of the D-T fusion reactions come from the thermal core, a fraction which increases to ~ 70% in the case of D-D plasmas owing to the higher plasma density in these cases. During the later evolved ITB phase, the steep plasma pressure profile produces a bootstrap current (up to ~ 30% of the total current) which serves to maintain the flattening of j(r). When the hot ion core forms, the centrally deposited ICRH power switches from predominantly hydrogen minority heating (which is coupled mainly to electrons) to direct bulk ion heating at second harmonic deuterium resonance. Variation of the ICRH power is used in real time to effectively control the plasma pressure profile in the confinement region. Up to 8.2 MW of D-T fusion power was produced in the H-mode and up to 7.2 MW in the L-mode. The fusion triple product reached values up to: $n\,\tau_E\,T = (1.1 \pm 0.2)\,10^{21}$ m^{-3} s keV in these plasmas.

Double barrier quasi-steady-state plasmas with superposed ITBs and an ELMy H-mode edge have also been produced and maintained for up to four energy replacement times. In D-T the fusion power reached P_{fus} = 7 MW in this mode and significant enhancements in fusion gain, Q, and ITER89-P normalised confinement were obtained over the standard ELMy sawtoothing H-mode plasma.

Based on the empirical JET transport scaling model with extra terms introduced to suppress turbulence, predictive modelling indicates the need to include the effects of both magnetic

and velocity shear to obtain agreement with experiment. Only in this way could both the growth rate and the size of the ITB be simulated adequately.

The optimisation of the ITB and double barrier discharges on JET is, however, not yet complete. Further work to do includes the following:

1) Increase the density in D-T plasmas by further optimisation of the NBI fuelling,
2) Control the plasma pressure profile in the confinement region and widen the ITB,
3) Control the edge pressure profile by gas puffing in the quest for quasi-steady-state, and
4) Control the current density profile using LHCD to increase the MHD stability .

REFERENCES

[1] Tubbing B. et al., Nuclear Fusion **31** (1991), 839.

[2] Hugon, M. et al., Nuclear Fusion **32** (1992), 33.

[3] Levington, F.M. et al., Phys. Rev. Lett. **75** (1995), 4417.

[4] Strait, E.J. et al., Phys. Rev. Lett. **75** (1995), 4421.

[5] Fujita,T. et al., Plasma Physics and Controlled Nuclear Fusion Research, Proc. 16th Int. Conf., Montreal, 1996, IAEA-CN-64/A1-4.

[6] Gormezano, C., et al. 1997 Plasma Physics and Controlled Nuclear Fusion Research, Proc. 16th Int. Conf., Montreal, 1996, IAEA-CN-64/A5-5.

[7] Sips, A.C.C. et al., Proc. 24th European Physical Society Conference on Controlled Fusion and Plasma Physics, Berchtesgaden, Germany, 1997. **21A(1)** 97 (1997).

[8] The JET Team (presented by Söldner, F.X.), Plasma Phys. and Controlled Fusion, **39** Supplement 12B (1997) B353

[9] Sips, A.C.C. et al., Plasma Phys. and Controlled Fusion, **40** (1998) 1171

[10] Gormezano, C. et al. Phys. Rev. Lett. **80** (1998), 5544.

[11] Huysmans, G.T.A. et al., Proc. 24th European Physical Society Conference on Controlled Fusion and Plasma Physics, Berchtesgaden, Germany, **21A(1)** 21 (1997).

[12] Cottrell, G.A., et al. Plasma Phys. and Controlled Fusion, **40** (1998) 1251

[13] Righi, E. et al. *Isotope Scaling of the H-mode Power Threshold in JET* submitted Nuclear Fusion (1998)

[14] Cottrell, G.A., et al. accepted Nuclear Fusion (1998)

[15] Hammett, G.W., "Fast Ion Studies of Ion Cyclotron Heating in PLT Tokamak", Ph.D Thesis, Princeton, USA, (1986).

[16] Mantsinen M., et al., Plasma Phys. and Controlled Fusion, to be published (1998)

[17] Mantsinen M., et al., Proc. 24th European Physical Society Conference on Controlled Fusion and Plasma Physics, Berchtesgaden, Germany, **21A(1)** 137 (1997).

[18] Stix, T.H., *Waves in Plasmas* American Institute of Physics, ISBN 0-88318-859-7 (1992)

[19] Söldner, F.X.et al., submitted Nuclear Fusion (1998)

[20] Hinton & Hazeltine 1976

[21] Lin et al. Physical Review Letters **78(3)** 458 (1997)

[22] Litaudon, X. et al., *Electron and ion internal transport barriers in Tore Supra and JET* Plasma Phys. and Controlled Fusion, to be published (1998)

[23] Parail, V.V., et al. 1998, Sub. to Nucl. Fusion